Assessment of the Coarse-Mesh Finite-Difference Method with the Multicell Methodology in RFSP for ACR-1000®[1]

W. Shen and B. Phelps
Atomic Energy of Canada Limited, Mississauga, Ontario, Canada
(shenwei@aecl.ca)

Abstract

Though the WIMS-AECL/RFSP-IST suite of codes has been in widespread use for design, safety and operational analysis over the years in the CANDU® industry, it is necessary to assess its adequacy for future CANDU applications, especially when new fuels and new reactors are under development. Use of the coarse-mesh finite-difference method in RFSP 2-group neutron-diffusion calculations has drawn particular attention from the designers and regulators, especially for the application to ACR-1000®. This paper presents assessment results between WIMS-AECL/RFSP (with various lattice sub-meshes with and without using the multicell methodology) and MCNP5 full-core calculation for the ACR-1000. The assessment results show that the agreement in the channel power between RFSP and MCNP is significantly improved when the multicell methodology is used in the RFSP calculations. The assessment also shows that the coarse-mesh finite-difference method (FDM) gives consistently smaller differences than the fine-mesh FDM. The reason for the better performance of the coarse-mesh FDM over the fine-mesh FDM is also discussed in the paper.

1. Introduction

The "standard" reactor-physics calculations for CANDU[2] and ACR-1000[3] reactors are based on separating the total neutronics problem into two or more level of analysis [1], one level of which is classified as the lattice calculation performed with WIMS-AECL [2] and the second level of which comprises the whole-core analysis with RFSP-IST (herein referred to as RFSP) [3] which applies lattice-homogenized properties based on the results of the lattice-cell and supercell calculations.

Though the WIMS-AECL/RFSP suite of codes has been in widespread use for design, safety and operational analysis over the years in the CANDU industry, it is necessary to assess its adequacy for future CANDU applications, especially when new fuels and new reactors are under development. In this paper, the assessment was made on the RFSP 2-group neutron-diffusion calculation results for the ACR-1000 core by using the coarse-mesh finite-difference method (FDM) with WIMS-AECL-based lattice-homogenized cross sections. Several sets of comparisons have been performed between WIMS-AECL/RFSP (with different lattice sub-meshes with and without using the multicell methodology) and MCNP5 [4] full-core results. These include WIMS-AECL/RFSP comparisons of channel powers for a 2-D 22x22 ACR benchmark problem, and for a snapshot of a 3D ACR-1000 full-core problem.

[2] CANDU is a registered trademark of Atomic Energy of Canada Limited (AECL).
[3] ACR-1000 is a registered trademark of Atomic Energy of Canada Limited (AECL).

2. Description of the benchmark problems

This section gives a brief description of the two benchmark problems used in the assessment.

2.1 2-D 22x22 ACR[4] benchmark problem

The 2-D 22x22 ACR benchmark problem consists of an 18x18 array of ACR fuel lattices, with a lattice pitch of 24 cm, surrounded by a two-lattice-pitch moderator-reflector boundary. The vacuum boundary condition was used at the four external surfaces in the XY plane and the reflective condition was used in the axial direction. Figure 1 illustrates the geometry. The fuel used in the benchmark problem is the ACR fuel and the fuel burnup was uniformly set at 8153 MWd/T to give an approximately critical core in MCNP.

2.2 ACR-1000 full-core problem

This is a snapshot of a 3-D ACR-1000 full-core problem with ACR-type fuels, heavy-water reflector and all in-core reactivity devices explicitly modeled. In order to perform an apples-to-apples comparison between WIMS/RFSP and MCNP for the ACR-1000 full-core problem, the following assumptions were used in the computational models:

- For simplicity and because of limitations in MCNP modelling, 72 different fuel irradiations were assigned to 6 radial (shown in Figure 2) and 12 axial fuel regions in both RFSP and MCNP full-core calculations;
- The same ring-wise fuel compositions, generated from WIMS depletion calculations. were used in both RFSP and MCNP full-core calculations;
- The guide tubes for the ZCU (Zone-Control Unit) were not modelled in either the RFSP or the MCNP full-core calculations;
- The axial end shield was not modelled and a vacuum boundary condition was applied in the axial direction in both RFSP and MCNP full-core calculations; and
- The variations of the local parameters across the core were also neglected. The local parameters were kept the same throughout the core in both RFSP and MCNP full-core calculations.

3. Description of the computational models

3.1 WIMS-AECL

WIMS-AECL is a 2-D multigroup neutron-transport code routinely used for reactor-physics calculations of CANDU and ACR lattices. It encompasses all neutronics aspects of lattice-cell calculations, from cross-section preparation to the cell homogenization and burnup calculation based on a detailed space-energy neutron-flux distribution. A new capability to handle general multi-cluster geometries with the collision-probability method has been developed at AECL in WIMS-AECL [5], which enables the use of multicell-based cross sections in RFSP. In other words, it is possible to use WIMS-AECL to generate lattice-cell cross sections that account for the neutronic coupling with the neighbour cells.

---

[4] ACR (Advanced CANDU Reactor) is a registered trademark of Atomic Energy of Canada Limited (AECL)

All WIMS calculations reported here were performed with WIMS-AECL version 3.1.2.1 [5]. The WIMS cross-section tables were generated with WIMS Utilities version 2.0.1 [6]. Both WIMS and WIMS Utilities were run on the PC Windows platform at AECL. The WIMS-AECL single-lattice-cell model and multicell model used in the calculations are shown in Figure 3. The WIMS-AECL multicell comprises an array of 10 lattice cells: four lattices are filled with heavy water to represent the reflector region and the remaining 6 lattices are regular ACR-type fuel bundles. The WIMS-AECL multicell calculation allows for the adjustment of the cross sections due to the neutron spectrum change for the periphery fuels at the core/reflector interface.

3.2 RFSP

RFSP is a 3D two-group neutron-diffusion code routinely used for reactor-physics calculations of CANDU and ACR cores. It uses the FDM to solve the neutron-diffusion equation. It does a wide variety of calculations, including time-average simulations for reactor design, time-dependent refuelling simulations, both slow (xenon transients) and fast (such as LOCA) kinetics calculations, control and shutdown system modelling, calculations of harmonic modes, flux detector responses and flux mapping. A new capability to use the multicell methodology to account for the effects of the environment has been developed at AECL in RFSP [7]. The multicell methodology allows a more accurate treatment of neutronic heterogeneity, while maintaining the basic structure of the single-lattice-cell-based reactor-physics methodology used for CANDU reactors.

All RFSP calculations reported here were performed with RFSP version 3.5 [7] on the LINUX platform at AECL. The channel flux/power calculations for the benchmark problems were performed with the static module *SIMULATE of RFSP. The two-group cross sections were generated with the micro-depletion method [8] with and without using the multicell methodology [9].

3.3 MINER

MINER (Multi-group Iterative Neutronics External Replacement) [10] is a 3-D multi-group neutron-diffusion code developed at AECL-SP. This package contains two multi-group diffusion solvers based on the FDM and GNEM (Green's Function Nodal Expansion Method) [11] methods. These solvers can be used in a stand-alone mode or can be plugged into RFSP. This allows MINER to use the RFSP core model directly. Consequently the 2-group diffusion equation can be solved with MINER on the RFSP core model.

Because of the limitation of a maximum of 100x100 meshes in the XY plane, RFSP cannot divide the lattice sub-meshes finer than 4x4 for the 22x22 ACR benchmark problem. Hence the stand-alone version of the MINER code was used to model the 22x22 ACR benchmark problem with the lattice sub-meshes finer than 4x4. The fuel and reflector cross sections were extracted from the micro-depletion tables generated beforehand with the WIMS-AECL single-cell model. Different spatial lattice sub-meshes were tested. Each cell in Figure 1 was either taken as one mesh or split into 2x2, 4x4, 8x8, and 12x12 meshes when the FDM was involved and as a single mesh when the GNEM was used.

3.4 MCNP

MCNP5 is a general-purpose Monte-Carlo N-Particle code used for neutron, photon, electron, or coupled neutron/photon/electron transport calculation. It can directly model arbitrary three-dimensional configuration of materials by using continuous energy libraries. The objective of the MCNP calculations is to provide reference solutions for the two benchmark problems described in the previous section.

All MCNP calculations [7] reported here were executed with MCNP Release 5 Version 1.30 [4] on the LINUX platform at AECL. To obtain statistically significant results for flux or power from a full core MCNP model is much more challenging than simply obtaining k-effective. Many more histories are required. For the 22x22 ACR benchmark problem, the MCNP results were calculated with 800 million histories. For the ACR-1000 full-core problem, the RFSP power distribution was used to obtain an initial source distribution for the MCNP calculation. The MCNP results were calculated with 1.5 billion histories.

4. Assessment results

Comparisons of WIMS-AECL/RFSP and MCNP channel powers for the two benchmark problems are presented in this section. The relative difference in the channel powers reported in this section is defined as:

$$\varepsilon_j = \left\{ \frac{P_j^{rfsp} - P_j^{mcnp}}{P_j^{mcnp}} \right\} \times 100\% \tag{1}$$

where P_j^{rfsp} is the RFSP-calculated channel power at channel location j and P_j^{mcnp} is the MCNP-calculated channel power at channel location j.

4.1 2-D 22x22 ACR benchmark problem

4.1.1 <u>RFSP results</u>

The RFSP channel powers calculated with 1x1, 2x2 and 4x4 lattice sub-meshes in the XY plane with and without using the multicell methodology were compared with the MCNP results. Figure 4 to Figure 6 show the differences in channel powers over the whole core between RFSP and MCNP with the following three calculation options, respectively:

- Option 1: 4x4 lattice sub-meshes in the XY plane without the multicell methodology
- Option 2: 4x4 lattice sub-meshes in the XY plane with the multicell methodology
- Option 3: 2x2 lattice sub-meshes in the XY plane with the multicell methodology

For all cases, the highest differences were observed at the edges where the fuel/reflector interface exists. This higher percentage difference is partially due to the fact that channel powers located around the outside edge of the core are of lower power and consequently an equivalent change in absolute power is a larger percentage than in the higher-power inner-core channels. As reported in Reference [7], the comparison of Figure 4 (option 1) and Figure 5 (option 2) shows that the agreement in the channel powers between RFSP and MCNP is significantly improved when the multicell methodology is used in the RFSP calculations: the maximum difference in the channel power reduced from ~3.6% to ~1.3% for the central high-power region. The comparison of Figure 5 (option 2) and Figure 6 (option 3) shows that the coarse-mesh (2x2) FDM gives smaller differences than the fine-mesh (4x4) FDM: the maximum difference in the channel power reduced from ~1.3% to ~1.0% for the central high-power region.

Table 1 summarizes the RFSP results of the 22x22 ACR benchmark problem with six calculation options. The table shows the maximum differences at the edge and central regions, the average difference as well as the RMS (Root Mean Square) differences for each calculation option. The comparison shows that the coarse mesh (1x1) FDM with the multicell methodology gives the best agreement with the MCNP results: maximum differences at the edge and the center are ~2.3% and ~0.5%, and the RMS difference is ~0.6%. Maximum differences are observed for the fine-mesh (4x4) FDM without the multicell methodology: maximum differences at the edge and the center are ~16.2% and ~3.6%, and the RMS difference is ~4.7%.

Though the 1x1 coarse-mesh FDM gives smallest differences compared to the MCNP results, it should be noted that once the in-core reactivity devices are represented (in the centre of neighbouring channels) in the CANDU or ACR-1000 core, at least 2x2 sub-meshes have to be used in RFSP calculations. Table 1 also shows that the 2x2 coarse-mesh FDM with the multicell methodology gives a very good agreement with the MCNP results: maximum differences at the edge (4 channels at the corner are excluded) and the center are ~3.6% and ~1.0%, and the RMS difference is ~1.3%.

4.1.2 MINER results

The results generated with MINER with both the FDM and GNEM methods were compared to the results calculated with MCNP. Table 2 summarizes the MINER results for FDM results with 1x1, 2x2, 4x4, 8x8, and 12x12 lattice sub-meshes and for GNEM with 1x1 lattice sub-mesh, respectively. The same observations and conclusion as above for the RFSP results can be made, i.e., the coarse-mesh FDM gives smaller differences than the fine-mesh FDM compared to the MCNP results. The coarse-mesh (1x1) nodal method produces results very close to those produced with the fine-mesh (8x8) FDM. As expected, the MINER produces almost identical results as the RFSP FDM results (without the multicell methodology) when the same lattice sub-meshes are used.

4.2 ACR-1000 full-core problem

The RFSP channel powers calculated with 2x2x2, 2x2x10 and 4x4x2[5] lattice sub-meshes in the X, Y, Z directions with and without using the multicell methodology were compared with the MCNP results. It should be noted that finer-mesh (such as 8x8 meshes in the XY plane) FDM calculations were not performed because of the limitation of the number of meshes in the XY plane in RFSP. Figure 7 to Figure 9 show the differences in the channel powers over the whole core between RFSP and MCNP with the following three calculation options, respectively:

- Option 1: 4x4x2 lattice sub-meshes in the X, Y, Z directions without the multicell methodology
- Option 2: 4x4x2 lattice sub-meshes in the X, Y, Z directions with the multicell methodology
- Option 3: 2x2x2 lattice sub-meshes in the X, Y, Z directions with the multicell methodology

5 Note that this is not a complete 4x4 lattice sub-meshes configuration in the XY plan. Some lattices have 2x2 sub-meshes in the XY plane.

As reported in Reference [7], the comparison of Figure 7 (option 1) and Figure 8 (option 2) shows that the agreement in the channel powers between RFSP and MCNP is significantly improved when the multicell methodology is used in the RFSP calculations: the maximum difference in the channel power reduced from ~6.2% to ~2.0% for the central high-power region. The comparison of Figure 8 (option 2) and Figure 9 (option 3) shows that the coarse-mesh (2x2x2) FDM gives smaller differences than the fine-mesh (4x4x2) FDM: the maximum difference in the channel powers reduced from ~2.0% to ~1.1% for the central high-power region.

Table 3 summarizes the RFSP results of the ACR-1000 full-core problem with six different calculation options. The table shows the maximum differences at the edge and central regions, the average difference as well as the RMS differences for each calculation option. As with the 2-D 22x22 ACR benchmark problem, it is seen that the coarse-mesh (2x2x2) FDM with the multicell methodology gives the best agreement with the MCNP results: maximum differences at the edge and the center are ~3.9% and ~1.1%, and the RMS difference is ~0.8%. Maximum differences are observed for the fine-mesh (4x4x2) FDM without the multicell methodology: maximum differences at the edge and the center are ~12.6% and ~6.2%, and the RMS difference is ~4.5%.

Figure 10 shows the differences in channel powers between RFSP (with four calculation options) and MCNP calculations for a row of channels across the core, channels N1 to N26. It clearly demonstrates that the 2x2x2 FDM with the multicell methodology gives the smallest differences in channel powers compared with the MCNP results. Compared with the 2x2x2 FDM results, the finer mesh used in the Z direction (option 2x2x10) also makes the results worse. Some abnormal fluctuation in the power shape is observed for the 2x2x10 FDM result, which is thought to be due to the use of device-homogenized cross sections for the non-device sub-mesh region in the Z direction as explained in the next sub-section.

Hence it is recommended to use 2 sub-meshes in X, Y, and Z directions with the FDM in RFSP for the ACR-1000 application.

4.3 Summary and discussions

Overall, the comparison of the RFSP and MCNP results shows consistency in the two benchmark problems that were considered in the assessment. The coarse-mesh FDM gives consistently smaller percent differences than the fine-mesh FDM compared to the reference MCNP solution.

The observed results may look abnormal at first glance because the fine-mesh FDM should give more accurate (i.e., spatially converged) results than the coarse-mesh FDM in theory. The better performance of the coarse-mesh FDM compared to that of the fine-mesh FDM might be considered a coincidence. However, after extensive sensitivity studies with different codes, different methods for different reactor types, it is concluded that this is not the case. It is thought that the bigger differences observed for the fine-mesh FDM are caused by the use of lattice-homogenized cross sections in the diffusion calculation. In fact, in the current homogenization technique, the lattice-cell properties are mixed to produce a single set of cross sections for any sub-mesh inside the lattice bundle. This is not an issue for LWR with the fine-mesh FDM because the LWR fuel assembly consists of uniformly distributed 17x17 fuel pins so that the fuel properties for different sub-meshes are not very different. However, this seems to be an issue for CANDU or ACR-1000 with the fine-mesh FDM because the fuel lattice-cell in both CANDU and ACR-1000 consists of a fuel cluster surrounded by tubes and heavy-water moderator so that the fuel properties for different sub-meshes are very different. Use of the fine-mesh FDM with a single set of cross sections for each sub-mesh in the fuel lattice-cell makes the results worse compared with MCNP. Use of the coarse-mesh FDM avoids this issue, with smaller cost on the spatial convergence of fluxes.

5. Conclusions

This paper presents assessment results between WIMS-AECL/RFSP (with various lattice sub-meshes with and without using the multicell methodology) and MCNP5 full-core calculations for the ACR-1000. The comparison of the RFSP and MCNP results shows consistency in the two benchmark problems that were considered in the assessment. The assessment results show that the agreement in the channel powers between RFSP and MCNP is significantly improved when the multicell methodology is used in the RFSP calculations. The assessment also shows that the coarse-mesh finite-difference method (FDM) gives smaller differences than the fine-mesh FDM compared to the MCNP results. It is recommended to use coarse-mesh (2x2x2 meshes/lattice bundle) FDM with the multicell methodology in RFSP for the ACR-1000 application, when the traditional lattice-homogenized cross sections are used in the diffusion calculation.

6. Acknowledgement

The authors wish to thank all reviewers, M. Dahmani and J. Hu in particular, for their careful and in-depth review of this paper. Thanks are also due to D.A. Jenkins, A. Connolly, I. Attieh, T. Liang and S. Hart who performed MCNP full-core calculations for benchmarking as reported in Reference [7], and to D. Buss, K. Ho and C. Gaver who helped on the RFSP/MCNP power comparisons reported in this paper.

7. References

[1] R. Roy, J. Koclas, W. Shen, D.A. Jenkins, D. Altiparmakov and B. Rouben, "Reactor Core Simulations in Canada", Proceedings of the International Conference on the Physics of Fuel Cycles and Advanced Nuclear Systems: Global Developments, PHYSOR 2004, Chicago, Illinois, April 25-29, 2004.

[2] J.D. Irish and S.R. Douglas, "Validation of WIMS-IST", Proceedings of the 23rd Annual Conference of Canadian Nuclear Society, Toronto, Canada, June 2-5, 2002.

[3] B. Rouben, "RFSP-IST, The Industry Standard Tool Computer Program for CANDU Reactor Core Design and Analysis", Proceedings of the 13th Pacific Basin Nuclear Conference, Shenzhen, China, Oct. 21-25, 2002.

[4] X5-MCNP-Team, "MCNP – A general Monte Carlo N-particle transport code, Version 5, Volume I: Overview and Theory", LA-UR-03-1987, Los Alamos National Laboratory, 2003.

[5] D. Altiparmakov, "New Capabilities of the Lattice Code WIMS-AECL", Proceedings of the International Conference on the Physics of Reactors "New Power: A Sustainable Resource", PHYSOR-2008, Interlaken, Switzerland, September 14-19, 2008.

[6] T. Liang, W. Shen, E. Varin and K. Ho, "Improvement and Qualification of WIMS Utilities", Proceedings of the 29th Annual Conference of Canadian Nuclear Society, Toronto, Ontario, Canada, June 1-4, 2008.

[7] W. Shen, D.A. Jenkins, A. Connolly, I. Attieh, D. Buss, T. Liang, and S. Hart, "Benchmarking of WIMS-AECL/RFSP Multicell Methodology with MCNP for ACR-1000 Full-Core Calculations", Proceedings of the International Conference on the Physics of Reactors "New Power: A Sustainable Resource", PHYSOR-2008, Interlaken, Switzerland, September 14-19, 2008.

[8] W. Shen, "Development of a Micro-Depletion Model to Use WIMS Properties in History-Based Local-Parameter Calculations in RFSP", Proceedings of the Sixth International Conference on Simulation Methods in Nuclear Engineering, Montreal, Canada, 2004 October 13-15.

[9] W. Shen, "Development of a Multicell Methodology to Account for Heterogeneous Core Effects in the Core-Analysis Diffusion Code" Proceedings of the International Conference on the Advances in Nuclear Analysis and Simulation, PHYSOR-2006, Vancouver, September 10-14, 2006.

[10] B. Phelps, W. Shen and E. Varin, "MINER: Three-Dimensional Multi-Group Finite-Difference and Nodal Method for CANDU Applications", Proceedings of the 30th Annual Conference of Canadian Nuclear Society, Calgary, Canada, May 31 - June 3, 2009.

[11] W. Shen, Z. Xie and B. Yin, "The Green's Function Nodal Expansion Method for Light Water Reactor Diffusion Calculations", Nucl. Sci. Eng., 121, 1995.

Table 1: Differences in channel powers between RFSP and MCNP for the 2-D 22X22 ACR benchmark problem

meshes/lattice	Multicell Method	E_{max} (Center)	E_{max} (Edge)	E_{avg}	E_{RMS}
1x1	No	-2.4%	9.4%	2.2%	2.9%
2x2	No	-3.2%	14.1%	3.1%	4.2%
4x4	No	-3.6%	16.2%	3.5%	4.7%
1x1	Yes	-0.5%	2.3%	0.4%	0.6%
2x2	Yes	-1.0%	7.0%	0.8%	1.3%
4x4	Yes	-1.3%	9.0%	1.1%	1.8%

Table 2: Differences in channel powers between MINER and MCNP for the 2-D 22X22 ACR benchmark problem

meshes/lattice	Multicell Method	E_{max} (Center)	E_{max} (Edge)	E_{avg}	E_{RMS}
1x1	FDM	-2.4%	9.2%	2.2%	2.8%
2x2	FDM	-3.2%	13.9%	3.0%	4.1%
4x4	FDM	-3.5%	15.9%	3.4%	4.7%
8x8	FDM	-3.8%	17.6%	3.7%	5.1%
12x12	FDM	-3.9%	17.9%	3.8%	5.2%
1x1	GNEM	-3.9%	18.3%	3.8%	5.3%

Table 3: Differences in channel powers between RFSP and MCNP for the ACR-1000 full-core problem

meshes/lattice bundle	Multicell Method	E_{max} (Center)	E_{max} (Edge)	E_{avg}	E_{RMS}
2x2x2	No	-4.9%	10.7%	2.8%	3.6%
2x2x10	No	-3.8%	8.9%	2.2%	2.8%
4x4x2	No	-6.2%	12.6%	3.5%	4.5%
2x2x2	Yes	-1.1%	3.9%	0.5%	0.8%
2x2x10	Yes	1.4%	-3.3%	0.7%	0.9%
4x4x2	Yes	-2.0%	6.5%	1.0%	1.4%

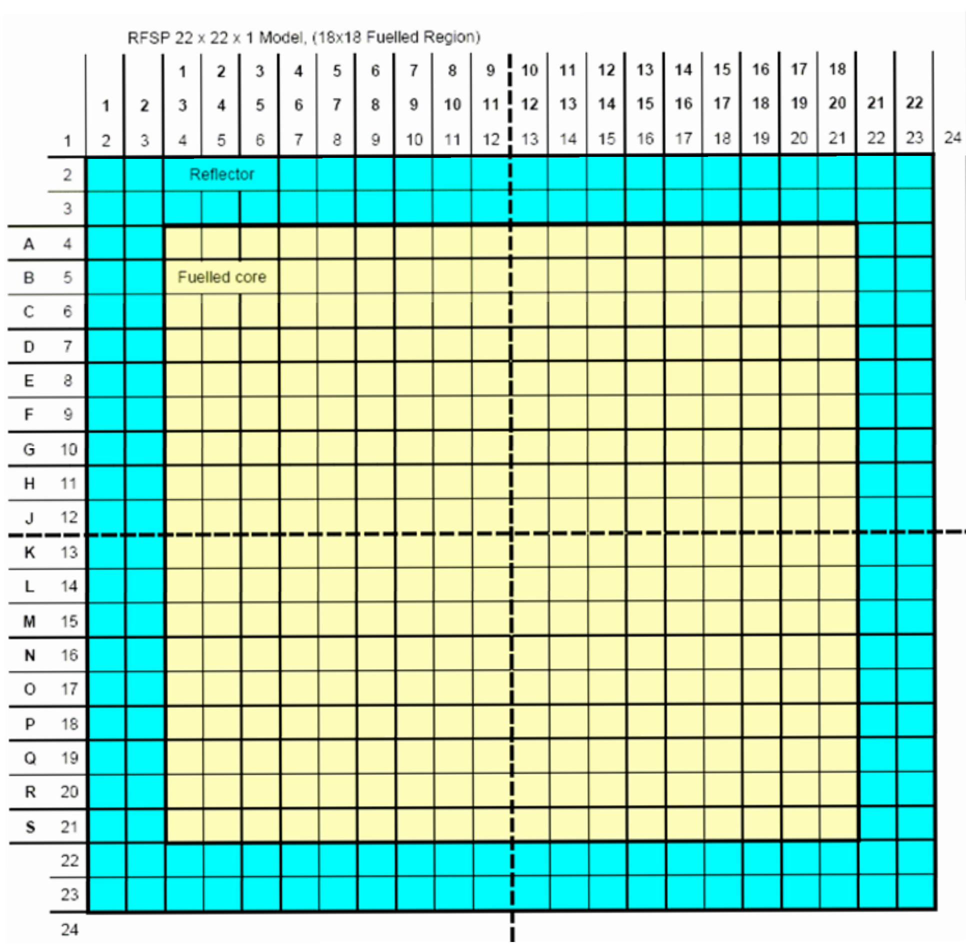

Figure 1: Illustration of the 2-D 22 x 22 ACR benchmark problem

	1	2	3	4	5	6	7	8	9	10	11	12	13	14	15	16	17	18	19	20	21	22	23	24	25	26
A											1	1	1	1	1	1										
B								1	1	1	1	2	2	2	2	1	1	1	1							
C							2	2	3	3	3	4	4	4	4	3	3	3	2	2						
D						2	2	3	3	4	4	4	5	5	4	4	4	3	3	2	2					
E				2	2	3	3	4	4	4	4	5	5	5	5	4	4	4	4	3	3	2	2			
F				3	4	4	4	4	4	5	5	5	6	6	5	5	5	4	4	4	4	4	3			
G			3	3	4	4	5	5	5	5	5	6	6	6	6	5	5	5	5	5	4	4	3	3		
H		1	3	4	5	5	5	5	5	5	5	5	6	6	5	5	5	5	5	5	5	5	4	3	1	
J		2	3	4	5	6	5	5	5	5	5	5	6	6	5	5	5	5	5	5	6	5	4	3	2	
K		2	4	5	6	6	5	5	5	5	5	6	6	6	6	5	5	5	5	5	6	6	5	4	2	
L	2	2	4	5	5	5	5	5	5	5	6	6	6	6	6	6	5	5	5	5	5	5	5	4	2	2
M	2	3	4	6	5	6	6	6	5	5	6	6	6	6	6	6	5	5	6	6	6	5	6	4	3	2
N	2	3	4	6	6	6	6	5	5	5	5	6	6	6	6	5	5	5	5	6	6	6	6	4	3	2
O	2	3	4	6	6	6	6	5	5	5	5	6	6	6	6	5	5	5	5	6	6	6	6	4	3	2
P	2	3	4	6	5	6	6	6	5	5	6	6	6	6	6	6	5	5	6	6	6	5	6	4	3	2
Q	2	2	4	5	5	5	5	5	5	5	6	6	6	6	6	6	5	5	5	5	5	5	5	4	2	2
R		2	4	5	6	6	5	5	5	5	5	6	6	6	6	5	5	5	5	5	6	6	5	4	2	
S		2	3	4	5	6	5	5	5	5	5	5	6	6	5	5	5	5	5	5	6	5	4	3	2	
T		1	3	4	5	5	5	5	5	5	5	5	6	6	5	5	5	5	5	5	5	5	4	3	1	
U			3	3	4	4	5	5	5	5	5	6	6	6	6	5	5	5	5	5	4	4	3	3		
V				3	4	4	4	4	4	5	5	5	6	6	5	5	5	4	4	4	4	4	3			
W				2	2	3	3	4	4	4	4	5	5	5	5	4	4	4	4	3	3	2	2			
X						2	2	3	3	4	4	4	5	5	4	4	4	3	3	2	2					
Y							2	2	3	3	3	4	4	4	4	3	3	3	2	2						
Z								1	1	1	1	2	2	2	2	1	1	1	1							
ZZ											1	1	1	1	1	1										

Figure 2 Illustration of six burnup zones used in the ACR-1000 full-core problem

a) WIMS-AECL Single-Lattice-Cell Model

b) WIMS-AECL Multicell Model for Core-Reflector Interface

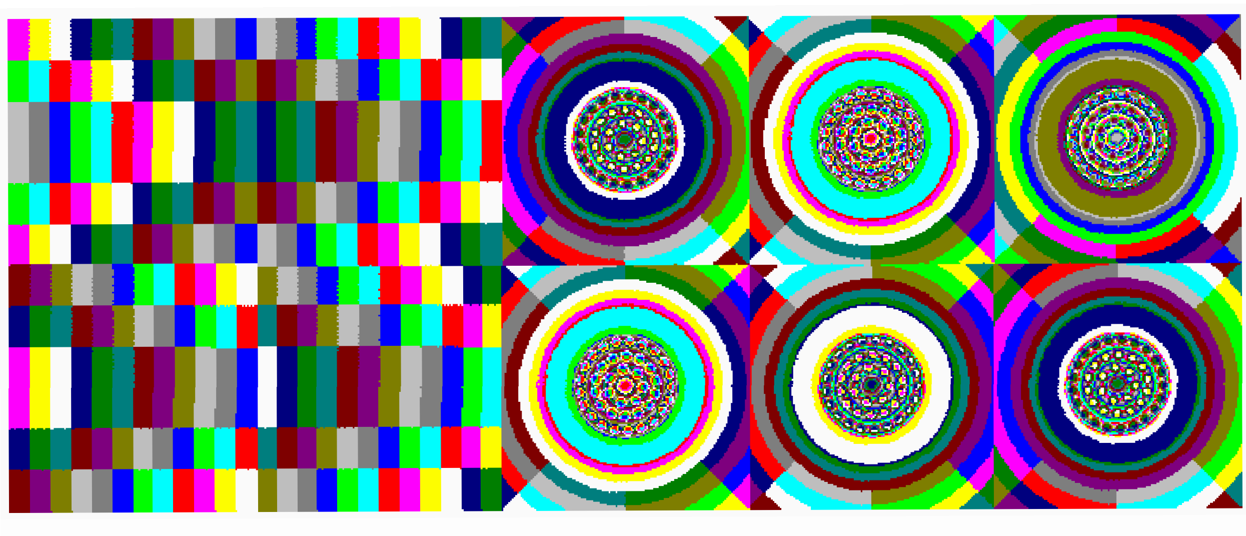

Figure 3 WIMS-AECL geometry model

	1	2	3	4	5	6	7	8	9	10	11	12	13	14	15	16	17	18
A	16.2	11.8	10.4	8.9	8.5	7.8	7.5	7.2	7.1	7.3	7.5	7.8	8.5	9.0	9.5	10.3	12.0	16.2
B	11.9	6.2	4.6	3.3	2.4	1.9	1.6	1.5	1.4	1.7	1.7	2.1	2.4	3.1	3.7	4.7	6.2	11.6
C	10.4	4.4	2.4	1.3	0.5	-0.1	-0.4	-0.3	-0.4	-0.4	-0.3	0.0	0.6	0.9	1.5	2.7	4.2	9.8
D	9.0	3.3	1.4	0.2	-0.6	-1.1	-1.4	-1.6	-1.6	-1.5	-1.3	-1.1	-0.7	-0.2	0.4	1.5	3.4	8.9
E	8.2	2.4	0.6	-0.6	-1.3	-1.9	-2.2	-2.4	-2.4	-2.3	-2.3	-1.8	-1.4	-1.1	-0.4	0.7	2.8	8.5
F	7.5	1.7	-0.1	-1.2	-1.8	-2.4	-2.7	-2.8	-2.9	-2.8	-2.5	-2.4	-2.1	-1.6	-0.7	0.5	2.5	8.2
G	7.0	1.5	-0.5	-1.5	-2.3	-2.7	-2.9	-3.0	-3.3	-3.2	-2.9	-2.8	-2.4	-1.9	-1.0	0.0	2.2	8.0
H	6.5	1.1	-0.8	-1.9	-2.7	-3.1	-3.3	-3.5	-3.5	-3.5	-3.2	-2.9	-2.5	-1.9	-1.3	0.1	2.0	7.9
J	6.4	0.9	-0.9	-2.0	-2.8	-3.3	-3.4	-3.4	-3.6	-3.6	-3.3	-3.0	-2.7	-2.0	-1.4	-0.1	2.2	7.8
K	6.4	1.0	-0.9	-2.1	-2.7	-3.3	-3.3	-3.6	-3.6	-3.6	-3.3	-3.1	-2.7	-2.2	-1.3	-0.2	1.9	7.7
L	6.5	0.9	-0.8	-1.8	-2.5	-3.0	-3.1	-3.4	-3.5	-3.5	-3.1	-2.9	-2.6	-2.0	-1.3	-0.1	2.1	8.0
M	7.0	1.1	-0.6	-1.7	-2.2	-2.8	-3.0	-3.0	-3.0	-3.1	-3.1	-2.6	-2.3	-1.8	-1.2	0.1	2.1	7.9
N	7.2	1.6	-0.4	-1.4	-1.9	-2.2	-2.6	-2.7	-2.8	-2.7	-2.5	-2.3	-2.0	-1.5	-0.8	0.2	2.4	8.3
O	7.5	1.8	-0.2	-1.0	-1.4	-1.8	-2.2	-2.3	-2.4	-2.2	-1.9	-1.7	-1.3	-0.9	-0.1	0.8	2.8	8.9
P	8.1	2.5	0.7	-0.4	-1.0	-1.2	-1.4	-1.5	-1.5	-1.5	-1.2	-0.9	-0.6	0.0	0.6	1.4	3.4	9.1
Q	8.9	3.3	1.8	0.6	-0.1	-0.2	-0.3	-0.4	-0.3	-0.1	0.1	0.3	0.7	1.1	1.7	2.7	4.3	9.8
R	10.7	4.9	3.4	2.5	2.1	1.7	1.7	1.7	1.7	1.8	2.1	2.4	2.7	3.1	3.7	4.5	6.0	11.6
S	14.9	10.8	9.2	8.1	7.6	7.4	7.4	7.5	7.5	7.7	7.7	8.1	8.3	8.8	9.4	10.2	11.8	16.1

Figure 4 Differences (%) in channel powers between RFSP (4x4 meshes/lattice without the multicell methodology) and MCNP calculations for the 2-D 22x22 ACR benchmark problem

	1	2	3	4	5	6	7	8	9	10	11	12	13	14	15	16	17	18
A	8.9	4.8	3.9	3.0	2.9	2.6	2.4	2.3	2.2	2.5	2.5	2.7	3.1	3.4	3.5	3.8	5.1	9.0
B	4.9	2.2	1.4	0.7	0.1	-0.1	-0.1	-0.1	-0.1	0.2	0.2	0.3	0.5	0.9	1.0	1.5	2.2	4.7
C	3.9	1.2	0.6	0.3	-0.1	-0.3	-0.4	-0.2	-0.2	-0.2	-0.2	-0.1	0.4	0.4	0.5	0.9	1.0	3.4
D	3.0	0.7	0.4	0.0	-0.2	-0.4	-0.5	-0.5	-0.4	-0.3	-0.3	-0.1	0.0	0.2	0.3	0.5	0.8	3.0
E	2.6	0.2	0.1	-0.2	-0.5	-0.7	-0.8	-0.8	-0.7	-0.6	-0.7	-0.4	-0.2	-0.2	0.0	0.1	0.6	2.9
F	2.2	-0.2	-0.3	-0.5	-0.6	-0.8	-0.9	-0.9	-0.9	-0.8	-0.5	-0.6	-0.5	-0.4	0.0	0.2	0.6	2.9
G	1.9	-0.2	-0.5	-0.6	-0.9	-0.9	-0.9	-0.8	-1.1	-0.9	-0.7	-0.8	-0.6	-0.4	-0.1	0.0	0.5	2.9
H	1.6	-0.5	-0.7	-0.9	-1.1	-1.1	-1.1	-1.2	-1.1	-1.1	-0.8	-0.7	-0.5	-0.3	-0.2	0.2	0.4	2.9
J	1.6	-0.6	-0.7	-0.9	-1.2	-1.3	-1.1	-1.0	-1.1	-1.1	-0.8	-0.7	-0.7	-0.4	-0.2	0.1	0.7	2.9
K	1.6	-0.6	-0.7	-1.0	-1.1	-1.3	-1.0	-1.1	-1.1	-1.1	-0.9	-0.8	-0.6	-0.5	-0.1	0.0	0.4	2.8
L	1.6	-0.7	-0.7	-0.8	-1.0	-1.0	-0.9	-1.1	-1.1	-1.0	-0.8	-0.7	-0.6	-0.4	-0.3	0.0	0.5	3.0
M	1.9	-0.6	-0.7	-0.7	-0.7	-1.0	-1.0	-0.8	-0.7	-0.8	-0.9	-0.5	-0.5	-0.4	-0.3	0.1	0.4	2.8
N	1.9	-0.3	-0.7	-0.7	-0.7	-0.6	-0.8	-0.7	-0.8	-0.6	-0.6	-0.5	-0.4	-0.3	-0.1	0.0	0.5	2.9
O	2.0	-0.4	-0.7	-0.6	-0.5	-0.6	-0.7	-0.7	-0.7	-0.5	-0.3	-0.2	-0.1	-0.1	0.3	0.3	0.6	3.2
P	2.2	-0.1	-0.3	-0.5	-0.6	-0.5	-0.4	-0.4	-0.4	-0.3	-0.2	0.0	0.0	0.4	0.4	0.4	0.7	3.1
Q	2.5	0.1	0.0	-0.4	-0.6	-0.4	-0.3	-0.3	-0.1	0.1	0.2	0.3	0.4	0.6	0.7	0.9	1.1	3.4
R	3.8	1.0	0.2	-0.1	-0.1	-0.2	0.0	0.1	0.2	0.3	0.5	0.7	0.7	0.9	1.0	1.3	2.1	4.7
S	7.8	3.9	2.8	2.2	2.1	2.1	2.4	2.5	2.6	2.8	2.8	3.0	3.0	3.2	3.4	3.7	4.8	8.9

Figure 5 Differences (%) in channel powers between RFSP (4x4 meshes/lattice with the multicell methodology) and MCNP calculations for the 2-D 22x22 ACR benchmark problem

	1	2	3	4	5	6	7	8	9	10	11	12	13	14	15	16	17	18
A	7.0	3.6	2.7	1.8	1.8	1.5	1.4	1.3	1.3	1.5	1.5	1.7	2.1	2.3	2.4	2.6	3.8	7.0
B	3.6	1.8	1.1	0.5	0.0	-0.2	-0.2	-0.2	-0.2	0.1	0.1	0.2	0.3	0.7	0.8	1.2	1.8	3.4
C	2.7	0.9	0.5	0.3	0.0	-0.2	-0.4	-0.1	-0.1	-0.1	-0.1	0.0	0.4	0.4	0.5	0.8	0.7	2.2
D	1.9	0.5	0.3	0.1	-0.2	-0.3	-0.4	-0.3	-0.2	-0.1	-0.1	0.0	0.2	0.3	0.3	0.4	0.5	1.9
E	1.6	0.0	0.1	-0.1	-0.3	-0.5	-0.5	-0.5	-0.5	-0.4	-0.4	-0.2	0.0	0.0	0.1	0.2	0.4	1.8
F	1.2	-0.4	-0.3	-0.3	-0.4	-0.6	-0.6	-0.6	-0.6	-0.5	-0.3	-0.3	-0.3	-0.2	0.1	0.3	0.4	1.9
G	0.9	-0.3	-0.4	-0.4	-0.7	-0.6	-0.6	-0.5	-0.8	-0.6	-0.4	-0.5	-0.3	-0.2	0.0	0.1	0.4	1.9
H	0.6	-0.6	-0.6	-0.7	-0.8	-0.8	-0.8	-0.8	-0.8	-0.7	-0.5	-0.4	-0.2	-0.1	-0.1	0.3	0.3	1.9
J	0.6	-0.7	-0.6	-0.7	-0.9	-1.0	-0.8	-0.7	-0.7	-0.7	-0.5	-0.4	-0.4	-0.1	-0.1	0.2	0.6	1.9
K	0.6	-0.6	-0.6	-0.8	-0.8	-1.0	-0.7	-0.8	-0.7	-0.7	-0.6	-0.5	-0.3	-0.3	0.0	0.1	0.3	1.8
L	0.6	-0.8	-0.6	-0.6	-0.7	-0.8	-0.6	-0.7	-0.7	-0.7	-0.5	-0.3	-0.3	-0.2	-0.1	0.1	0.4	2.0
M	0.9	-0.7	-0.6	-0.6	-0.5	-0.7	-0.7	-0.5	-0.4	-0.5	-0.6	-0.2	-0.3	-0.2	-0.1	0.2	0.2	1.7
N	0.9	-0.5	-0.6	-0.6	-0.5	-0.4	-0.5	-0.4	-0.5	-0.3	-0.3	-0.2	-0.2	-0.1	0.0	0.1	0.3	1.9
O	0.9	-0.6	-0.7	-0.5	-0.4	-0.4	-0.5	-0.4	-0.5	-0.3	-0.1	0.0	0.1	0.1	0.3	0.3	0.4	2.1
P	1.1	-0.4	-0.4	-0.5	-0.6	-0.4	-0.3	-0.3	-0.2	-0.2	0.0	0.2	0.2	0.4	0.4	0.4	0.5	2.0
Q	1.3	-0.2	-0.1	-0.4	-0.6	-0.4	-0.2	-0.2	0.0	0.2	0.3	0.4	0.5	0.6	0.7	0.8	0.8	2.2
R	2.5	0.6	-0.1	-0.4	-0.3	-0.4	-0.1	0.0	0.1	0.2	0.4	0.5	0.6	0.7	0.8	1.0	1.6	3.3
S	5.8	2.6	1.6	1.1	1.0	1.1	1.4	1.6	1.6	1.9	1.8	2.0	1.9	2.1	2.3	2.5	3.5	6.9

Figure 6 Differences (%) in channel powers between RFSP (2x2 meshes/lattice with the multicell methodology) and MCNP calculations for the 2-D 22x22 ACR benchmark problem

	1	2	3	4	5	6	7	8	9	10	11	12	13	14	15	16	17	18	19	20	21	22	23	24	25	26
A											10.6	10.0	10.0	10.5	10.9	11.9										
B								10.3	8.8	7.3	4.9	4.2	4.3	4.7	5.1	6.0	8.9	10.6	12.0							
C							8.1	4.9	3.8	3.4	2.8	2.6	2.4	2.4	2.9	3.5	4.6	5.2	6.5	10.2						
D						8.1	4.4	2.2	1.6	1.4	1.4	1.2	1.2	0.8	1.3	1.9	2.5	2.9	3.8	5.5	9.4					
E				11.8	7.2	4.2	2.3	1.3	0.5	0.2	0.2	-0.1	-0.2	-0.2	-0.2	0.6	1.2	1.5	2.3	3.3	4.8	8.1	12.6			
F				8.2	4.3	2.1	0.9	0.0	-0.7	-0.9	-1.4	-1.5	-1.8	-1.7	-1.3	-0.8	-0.3	0.2	0.9	1.7	2.7	4.5	8.6			
G			9.1	4.7	2.4	1.1	-0.1	-1.3	-1.6	-1.8	-2.3	-2.8	-3.0	-2.8	-2.4	-2.1	-1.8	-1.1	-0.6	0.3	1.0	2.4	4.5	9.1		
H		9.6	5.3	2.5	1.2	0.0	-1.3	-2.0	-2.5	-2.9	-3.4	-3.3	-3.8	-3.4	-3.6	-2.9	-2.4	-2.1	-1.7	-0.6	0.1	1.2	2.4	5.1	9.5	
J		8.9	3.6	1.7	0.2	-1.0	-2.1	-2.7	-3.6	-3.9	-4.1	-4.2	-4.5	-4.7	-4.1	-4.0	-3.4	-2.9	-2.5	-1.5	-0.9	0.4	1.5	3.2	8.6	
K		6.7	2.6	0.8	-0.4	-1.6	-2.2	-3.2	-4.0	-4.7	-4.7	-4.7	-5.1	-5.2	-5.0	-4.6	-4.2	-3.5	-2.9	-2.2	-1.2	-0.3	1.4	3.1	7.7	
L	10.0	4.2	1.7	0.2	-0.7	-2.0	-2.7	-3.8	-4.3	-4.8	-5.0	-5.0	-5.2	-5.4	-5.4	-5.1	-4.6	-4.2	-3.7	-2.9	-2.0	-0.5	1.0	2.8	5.0	10.8
M	9.0	3.1	1.0	-0.3	-1.1	-2.4	-3.1	-3.7	-4.3	-5.0	-5.2	-5.3	-5.7	-5.6	-5.4	-5.6	-5.1	-4.8	-4.2	-3.2	-2.3	-1.5	0.1	1.7	3.8	10.1
N	8.4	2.6	0.5	-0.6	-1.2	-2.3	-3.0	-3.6	-4.1	-4.7	-5.2	-5.3	-5.6	-6.0	-6.1	-5.8	-5.5	-5.2	-4.7	-3.6	-2.6	-1.5	0.0	1.1	3.3	9.8
O	8.3	2.4	0.6	-0.5	-1.5	-2.3	-3.2	-3.7	-4.3	-5.1	-5.6	-5.9	-5.8	-5.9	-6.2	-5.8	-5.5	-5.1	-4.6	-4.1	-2.9	-1.6	-0.5	0.9	3.0	9.0
P	8.4	2.7	0.8	-1.0	-1.5	-2.5	-2.9	-3.8	-4.1	-4.7	-5.4	-5.6	-6.0	-5.9	-5.8	-5.9	-5.7	-5.2	-4.8	-3.8	-2.8	-1.8	-0.5	1.0	3.2	8.7
Q	8.6	3.5	0.9	-0.7	-1.5	-2.4	-2.8	-3.6	-3.9	-4.4	-5.0	-5.4	-5.8	-6.0	-6.0	-5.8	-5.3	-5.1	-4.6	-3.6	-2.6	-1.6	-0.3	1.5	4.4	9.5
R		6.0	1.5	0.0	-1.1	-2.2	-2.6	-3.0	-3.6	-4.3	-4.7	-5.0	-5.3	-5.3	-5.2	-5.5	-4.9	-4.4	-3.9	-3.0	-2.2	-1.1	0.0	2.0	6.4	
S		7.6	2.3	0.7	-0.3	-1.3	-1.8	-2.7	-3.2	-3.7	-4.1	-4.5	-4.9	-4.8	-4.7	-4.5	-4.3	-3.9	-3.1	-2.2	-1.6	-0.6	0.5	2.8	8.2	
T		8.2	3.7	1.5	0.4	-0.2	-1.1	-2.1	-2.5	-3.2	-3.5	-3.6	-4.1	-4.0	-3.9	-3.6	-3.5	-3.0	-2.4	-1.3	-0.5	0.5	1.8	4.4	9.0	
U			7.7	3.4	1.7	0.5	-0.6	-1.0	-2.1	-2.4	-2.5	-3.0	-3.4	-3.2	-3.1	-3.0	-2.6	-2.0	-1.1	-0.7	0.4	1.8	3.8	7.9		
V				7.3	3.5	1.8	0.6	-0.1	-0.7	-1.3	-1.9	-2.2	-2.3	-2.3	-2.2	-2.1	-1.9	-1.1	-0.3	0.7	1.8	3.6	7.4			
W				11.2	7.0	4.4	2.4	1.5	0.6	-0.1	-0.6	-0.8	-1.3	-1.5	-1.1	-0.8	-0.8	0.1	0.6	1.9	4.1	6.5	10.8			
X						8.7	4.6	2.6	1.8	0.9	0.4	0.5	0.1	-0.2	0.2	0.5	0.6	1.2	1.9	4.1	7.6					
Y							8.8	5.1	3.6	2.8	2.2	2.1	1.4	1.1	1.7	1.9	2.8	3.6	4.9	8.1						
Z								9.2	8.5	7.0	4.4	4.2	3.8	3.4	3.9	4.4	7.2	8.3	9.7							
ZZ											10.2	9.6	9.0	8.6	8.8	8.9										

Figure 7 Differences (%) in channel powers between RFSP (4x4x2 meshes/lattice bundle without the multicell methodology) and MCNP calculations for the 3D ACR-1000 full-core problem

	1	2	3	4	5	6	7	8	9	10	11	12	13	14	15	16	17	18	19	20	21	22	23	24	25	26
A											3.9	3.1	3.0	3.5	3.9	5.1										
B								4.1	2.4	1.1	1.1	0.5	0.6	1.0	1.3	2.2	2.6	4.1	5.7							
C							2.3	1.6	0.6	0.6	0.8	0.8	0.7	0.7	1.1	1.4	1.7	2.0	3.1	4.3						
D						2.5	1.6	0.4	0.2	0.4	0.8	0.8	0.9	0.5	0.9	1.3	1.5	1.6	2.0	2.7	3.8					
E				5.7	1.3	1.5	0.8	0.7	0.4	0.4	0.6	0.5	0.5	0.5	0.5	1.0	1.4	1.4	1.7	1.8	2.2	2.2	6.5			
F				2.2	1.5	0.7	0.5	0.2	0.0	0.1	0.0	0.0	-0.2	-0.1	0.2	0.6	0.8	0.9	1.2	1.3	1.4	1.7	2.7			
G			3.1	1.7	0.9	0.6	0.2	-0.3	-0.2	0.0	-0.3	-0.6	-0.6	-0.5	-0.2	-0.1	0.1	0.4	0.4	0.7	0.7	0.9	1.7	3.2		
H		3.3	1.8	0.6	0.5	0.2	-0.4	-0.5	-0.5	-0.5	-0.7	-0.5	-0.9	-0.5	-0.7	-0.2	0.0	0.0	-0.1	0.4	0.3	0.6	0.5	1.7	3.3	
J		2.4	0.4	0.3	0.1	-0.3	-0.7	-0.7	-1.2	-1.0	-0.9	-0.9	-1.1	-1.3	-0.8	-0.8	-0.4	-0.4	-0.5	0.0	-0.2	0.3	0.2	0.0	2.2	
K		0.5	-0.2	-0.2	-0.2	-0.5	-0.4	-0.9	-1.1	-1.4	-1.2	-1.0	-1.2	-1.4	-1.2	-1.0	-0.9	-0.5	-0.5	-0.3	-0.1	0.0	0.4	0.3	1.4	
L	3.3	0.5	-0.3	-0.4	-0.3	-0.7	-0.6	-1.2	-1.1	-1.3	-1.2	-1.0	-1.1	-1.2	-1.3	-1.2	-1.0	-1.1	-1.0	-0.7	-0.6	0.0	0.5	0.9	1.4	4.2
M	2.2	-0.4	-0.7	-0.6	-0.4	-0.9	-0.8	-0.9	-0.9	-1.2	-1.2	-1.1	-1.4	-1.3	-1.2	-1.6	-1.3	-1.4	-1.4	-0.9	-0.7	-0.7	-0.2	0.1	0.3	3.3
N	1.6	-0.9	-1.0	-0.9	-0.5	-0.7	-0.6	-0.6	-0.7	-0.9	-1.1	-1.0	-1.2	-1.6	-1.7	-1.7	-1.6	-1.8	-1.7	-1.2	-0.9	-0.6	-0.1	-0.4	-0.2	2.9
O	1.5	-1.1	-0.9	-0.7	-0.8	-0.7	-0.8	-0.8	-0.8	-1.2	-1.5	-1.6	-1.4	-1.5	-1.8	-1.7	-1.6	-1.7	-1.7	-1.7	-1.3	-0.8	-0.6	-0.6	-0.4	2.2
P	1.6	-0.8	-0.9	-1.3	-0.9	-1.0	-0.7	-1.0	-0.8	-1.0	-1.4	-1.4	-1.6	-1.6	-1.6	-1.8	-1.9	-1.8	-1.9	-1.5	-1.2	-1.1	-0.8	-0.6	-0.3	2.0
Q	2.1	-0.1	-1.0	-1.2	-1.0	-1.0	-0.7	-0.9	-0.7	-0.8	-1.1	-1.3	-1.7	-1.9	-1.9	-2.0	-1.8	-1.9	-1.9	-1.5	-1.2	-1.1	-0.8	-0.4	0.8	2.9
R		-0.2	-1.3	-1.0	-0.8	-1.1	-0.8	-0.5	-0.7	-1.0	-1.1	-1.2	-1.4	-1.4	-1.4	-1.9	-1.6	-1.5	-1.4	-1.1	-1.1	-0.8	-0.9	-0.7	0.3	
S		1.2	-0.8	-0.7	-0.4	-0.5	-0.4	-0.6	-0.6	-0.8	-0.9	-1.2	-1.4	-1.3	-1.3	-1.3	-1.3	-1.3	-1.1	-0.7	-0.8	-0.6	-0.7	-0.3	1.9	
T		2.0	0.3	-0.4	-0.2	0.1	-0.2	-0.5	-0.4	-0.8	-0.7	-0.7	-1.1	-1.0	-1.0	-0.9	-1.1	-0.9	-0.8	-0.3	-0.2	0.0	0.0	1.0	2.9	
U			1.8	0.5	0.2	0.1	-0.2	0.0	-0.6	-0.5	-0.4	-0.7	-1.0	-0.8	-0.8	-0.9	-0.7	-0.5	-0.1	-0.2	0.1	0.5	1.0	2.0		
V				1.4	0.7	0.5	0.3	0.2	0.1	-0.2	-0.5	-0.7	-0.7	-0.7	-0.6	-0.6	-0.7	-0.3	0.1	0.4	0.6	0.9	1.6			
W				5.2	1.2	1.7	1.0	0.9	0.5	0.1	-0.1	-0.1	-0.5	-0.7	-0.4	-0.2	-0.5	0.0	0.1	0.6	1.5	0.8	4.8			
X						3.2	1.9	0.9	0.5	0.0	-0.1	0.2	-0.2	-0.4	-0.1	0.0	-0.3	0.0	0.2	1.5	2.1					
Y							3.1	1.8	0.5	0.0	0.2	0.4	-0.2	-0.5	0.0	0.0	0.0	0.5	1.7	2.4						
Z								3.1	2.3	0.9	0.8	0.6	0.2	-0.2	0.3	0.8	1.1	2.0	3.6							
ZZ											3.7	2.8	2.2	1.8	2.1	2.5										

Figure 8 Differences (%) in channel powers between RFSP (4x4x2 meshes/lattice bundle with the multicell methodology) and MCNP calculations for the 3D ACR-1000 full-core problem

	1	2	3	4	5	6	7	8	9	10	11	12	13	14	15	16	17	18	19	20	21	22	23	24	25	26
A											2.7	1.8	1.8	2.3	2.6	3.9										
B								1.8	0.0	-0.9	0.5	0.2	0.3	0.7	1.0	1.5	0.5	1.7	3.4							
C							0.4	0.6	-0.1	0.1	0.5	0.7	0.6	0.6	1.0	1.1	1.2	1.3	2.0	2.4						
D						0.6	0.7	0.0	0.0	0.2	0.7	0.8	1.0	0.5	1.0	1.2	1.3	1.3	1.5	1.8	1.8					
E				2.3	-0.5	0.6	0.3	0.4	0.2	0.4	0.8	0.8	0.8	0.8	0.7	1.2	1.4	1.3	1.4	1.3	1.3	0.4	3.1			
F				-0.3	0.6	0.2	0.3	0.2	0.2	0.4	0.4	0.5	0.3	0.4	0.7	1.0	1.1	1.1	1.1	1.0	0.8	0.8	0.1			
G			0.9	0.7	0.2	0.3	0.1	-0.2	0.1	0.4	0.3	0.1	0.1	0.2	0.5	0.5	0.6	0.7	0.5	0.6	0.3	0.3	0.6	1.0		
H		1.0	0.7	0.0	0.1	0.1	-0.2	-0.1	0.1	0.1	0.0	0.4	0.0	0.4	0.2	0.5	0.7	0.5	0.3	0.6	0.2	0.2	-0.1	0.5	0.9	
J		-0.2	-0.4	-0.1	-0.1	-0.3	-0.3	-0.2	-0.5	-0.2	0.0	0.1	0.0	-0.3	0.2	0.1	0.4	0.3	0.0	0.3	-0.1	0.1	-0.3	-0.8	-0.4	
K		-1.7	-0.8	-0.4	-0.2	-0.3	0.1	-0.2	-0.3	-0.5	-0.1	0.1	-0.1	-0.3	-0.1	0.0	0.1	0.3	0.1	0.1	0.2	0.0	0.2	-0.3	-0.8	
L	2.0	-0.3	-0.7	-0.5	-0.2	-0.3	-0.1	-0.4	-0.2	-0.3	-0.1	0.2	0.1	0.0	-0.1	-0.1	0.0	-0.2	-0.2	-0.2	-0.2	0.1	0.3	0.5	0.6	2.9
M	0.8	-0.9	-0.9	-0.7	-0.2	-0.4	-0.2	0.0	0.0	-0.2	0.0	0.1	-0.1	0.0	0.0	-0.4	-0.2	-0.5	-0.6	-0.3	-0.3	-0.6	-0.3	-0.1	-0.1	1.8
N	0.2	-1.3	-1.2	-0.9	-0.2	-0.3	0.0	0.2	0.3	0.2	0.1	0.3	0.1	-0.3	-0.5	-0.5	-0.5	-0.8	-0.9	-0.6	-0.5	-0.4	-0.1	-0.6	-0.5	1.5
O	0.1	-1.4	-1.1	-0.7	-0.6	-0.2	-0.2	0.1	0.2	-0.1	-0.3	-0.3	-0.1	-0.2	-0.6	-0.5	-0.5	-0.7	-0.8	-1.0	-0.8	-0.6	-0.6	-0.7	-0.8	0.8
P	0.1	-1.2	-1.1	-1.3	-0.7	-0.6	0.0	-0.2	0.2	0.1	-0.2	-0.1	-0.4	-0.3	-0.3	-0.7	-0.8	-0.9	-1.1	-0.9	-0.8	-0.9	-0.8	-0.8	-0.7	0.5
Q	0.8	-0.9	-1.4	-1.4	-0.9	-0.7	-0.1	-0.2	0.2	0.2	0.0	-0.2	-0.5	-0.7	-0.7	-0.9	-0.7	-1.0	-1.1	-0.9	-0.8	-1.0	-0.9	-0.8	0.0	1.6
R		-2.3	-1.9	-1.2	-0.9	-0.8	-0.3	0.1	0.1	-0.1	-0.1	-0.1	-0.3	-0.3	-0.3	-0.9	-0.7	-0.7	-0.8	-0.7	-0.8	-0.9	-1.2	-1.3	-1.9	
S		-1.3	-1.6	-1.1	-0.6	-0.4	-0.1	-0.1	0.1	0.0	0.0	-0.2	-0.4	-0.3	-0.3	-0.4	-0.5	-0.7	-0.5	-0.4	-0.7	-0.8	-1.1	-1.1	-0.7	
T		-0.4	-0.8	-1.0	-0.6	0.0	0.0	-0.1	0.1	-0.1	0.0	0.1	-0.3	-0.2	-0.1	-0.1	-0.4	-0.4	-0.4	-0.1	-0.3	-0.4	-0.6	-0.1	0.5	
U			-0.3	-0.5	-0.4	-0.2	-0.2	0.2	-0.3	0.0	0.2	0.0	-0.3	-0.1	-0.2	-0.3	-0.2	-0.2	0.1	-0.3	-0.2	-0.2	-0.1	-0.1		
V				-1.1	-0.2	-0.1	0.0	0.2	0.2	0.1	-0.1	-0.2	-0.2	-0.2	-0.1	-0.3	-0.4	-0.1	0.0	0.1	0.0	0.0	-1.0			
W				1.8	-0.6	0.8	0.5	0.6	0.4	0.2	0.1	0.1	-0.2	-0.4	-0.1	-0.1	-0.4	-0.1	-0.2	0.0	0.6	-1.0	1.4			
X						1.2	1.0	0.4	0.2	-0.2	-0.2	0.2	-0.1	-0.4	-0.1	-0.1	-0.5	-0.3	-0.2	0.6	0.2					
Y							1.2	0.8	-0.2	-0.5	-0.1	0.3	-0.3	-0.6	-0.2	-0.3	-0.5	-0.2	0.7	0.5						
Z								0.8	-0.1	-1.1	0.1	0.2	-0.1	-0.4	0.0	0.1	-1.0	-0.4	1.3							
ZZ											2.5	1.5	1.0	0.7	0.8	1.3										

Figure 9 Differences (%) in channel powers between RFSP (2x2x2 meshes/lattice bundle with the multicell methodology) and MCNP calculations for the 3D ACR-1000 full-core problem

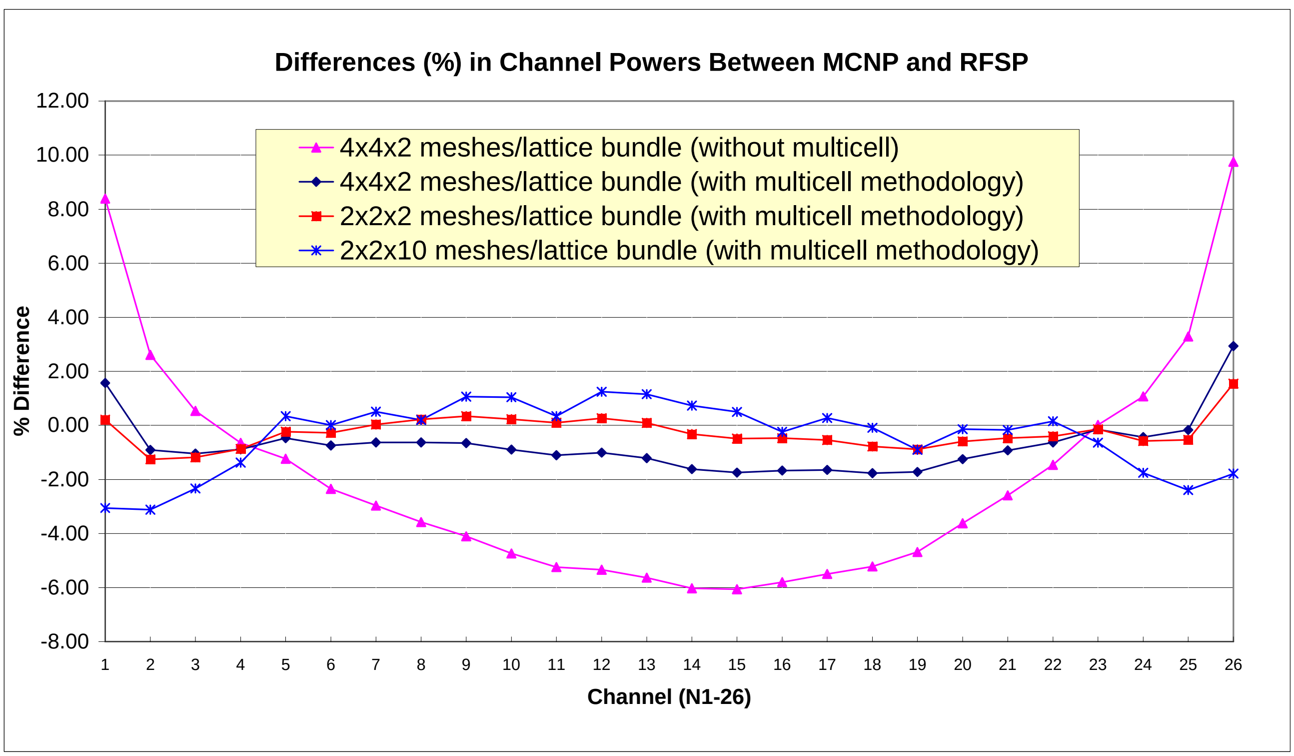

Figure 10 Differences (%) in channel powers between RFSP and MCNP calculations for the 3D ACR-1000 full-core problem